

# A POLYNOMIAL APPROXIMATION SCHEME FOR NONLINEAR MODEL REDUCTION BY MOMENT MATCHING\*

CARLOS DOEBELI<sup>†</sup>, ALESSANDRO ASTOLFI<sup>‡</sup>, DANTE KALISE<sup>†</sup>, ALESSIO MORESCHINI<sup>‡</sup>, GIORDANO SCARCIOTTI<sup>‡</sup>, AND JOEL SIMARD<sup>‡</sup>

**Abstract.** We propose a procedure for the numerical approximation of invariance equations arising in the moment matching technique associated with reduced-order modeling of high-dimensional dynamical systems. The Galerkin residual method is employed to find an approximate solution to the invariance equation using a Newton iteration on the coefficients of a monomial basis expansion of the solution. These solutions to the invariance equations can then be used to construct reduced-order models. We assess the ability of the method to solve the invariance PDE system as well as to achieve moment matching and recover a system’s steady-state behaviour for linear and nonlinear signal generators with system dynamics up to  $n = 1000$  dimensions.

**Key words.** reduced-order modeling, moment matching, invariance equations, global polynomial approximation

**AMS subject classifications.** 49M15, 70Q05, 93A30

**1. Introduction.** Complex large-scale dynamical systems are ubiquitous in control engineering. They provide a natural framework to model multi-agent systems, energy networks, and coupled systems of electrical signals, to name a few [25]. The high dimensionality of these models, often in the order of thousands or millions of states, introduces significant computational challenges when trying to analyse the behaviour of such systems, a phenomenon known as the “curse of dimensionality” [9]. The curse of dimensionality naturally appears in control systems design where it is often the case that the resulting control law has a complexity that is proportional, or worse, to the complexity of the system being controlled. This occurs in state feedback and observer design, where the controller is of proportional dimension to the system; model predictive control, where an optimization problem is run on the model at every time step to determine a cost-minimizing control input, and adaptive control, where different parameters need to be estimated while constructing a control input. Such control methods may be infeasible or costly to implement in practice when applied directly to the high-dimensional model. Therefore, it is often beneficial to reduce the complexity of the model by making approximations that make the problem easier and more tractable to solve, while maintaining accuracy and/or particular properties of the system.

Reduced-order modeling aims to alleviate the computational complexity of a problem while preserving important characteristics, creating a smaller model that approximates the behaviour of a complex system to some prescribed degree of accuracy. Reduced-order modeling finds application in the analysis and design of systems in many fields, for example mechanical and electrical systems, and weather forecasting [11, 2]. Broadly speaking, model order reduction methods are categorized as being based upon the singular value decomposition, such as Balanced Truncation [27, 26, 38] and Proper Orthogonal Decomposition [28, 29, 42], or as being based upon the no-

---

\*Submitted to the editors December 13, 2024.

<sup>†</sup>Department of Applied Mathematics, Imperial College London (c.doebeli22@imperial.ac.uk, d.kalise-balza@imperial.ac.uk)

<sup>‡</sup>Department of Electrical and Electronic Engineering, Imperial College London (j.simard18@imperial.ac.uk, a.moreschini@imperial.ac.uk, a.astolfi@imperial.ac.uk, g.scarciotti@imperial.ac.uk)

tion of Krylov projection/interpolation, such as moment matching [4, 3], see [1] for a comprehensive overview. Other approaches for model order reduction include energy-based methods [16, 37], reduction around a limit cycle [17], and transfer function interpolation for polynomial systems [10].

In this article, we focus on nonlinear model reduction by moment matching for interconnected systems involving a signal generator and a nonlinear system, building on the theory of output regulation. For recent surveys of techniques in reduced-order modeling by moment matching see *e.g.* [33, 36]. For linear systems, the concept of moment matching was shown to be in one-to-one relation with the solution to a Sylvester equation and an associated manifold induced by the interconnection of the system and the signal generator [15]. With additional stability assumptions the invariant manifold is attractive, and the solution of the Sylvester equation can further linked to the steady-state response [21]. This relationship was enhanced for nonlinear systems in [20], where the notion of invariance was associated with the solution of a ‘‘Sylvester-like’’ high-dimensional system of nonlinear coupled PDEs. With additional (local) stability assumptions, the invariant manifold associated to the solution of the PDE system is (locally) attractive and, similarly to the linear case, can be related to the notion of steady-state response. This enables the definition of moment matching to be decoupled from the inherently linear concept of frequency response, and [4] generalized the notion of moment matching to nonlinear systems by considering the invariant manifold induced by interconnection of nonlinear systems which is the solution to a PDE system of the form studied in this article.

The interconnection-based interpretation of moment matching presented in [4] leads to many further developments in the theory of moment matching. For nonlinear systems this includes, for example, the two-sided nonlinear moment matching framework [19], a data-driven approach for estimation of the moment of a nonlinear system by fitting a linear combination of basis functions to observed steady-state trajectories [35, 31], the parametrization of all differential-algebraic systems that achieve moment matching [39, 40], and the closed-loop moment matching framework that allows for the relaxation of the stability requirement on the system to be interpolated in the time domain [30]. A recent survey on interconnection-based model order reduction is provided in [36].

The notion of invariance commonly arises in control theory and the analysis of dynamical systems, so PDE systems of the form considered here are ubiquitous and not unique to the problem of model reduction. The output regulation problem for nonlinear control systems requires the solution of a system of PDEs corresponding to an invariance condition [12]. Control design via immersion and invariance was introduced in [5], where the solution to the PDE system is an immersion of the dynamics of the system-to-be-controlled into those of a ‘‘target system’’ having desired closed-loop behaviour, and the solution to the PDE system is used to construct a controller which achieves this closed-loop behaviour in steady-state.

At this point, the main limitation of the proposed method is that it requires numerical approximation of a large-scale system of coupled nonlinear PDEs over a domain that is determined by the dimension of the signal generator. Overall, for an  $n$ -dimensional dynamical system and a  $d$ -dimensional signal generator, we need to solve a system of  $nd$  PDEs in  $\mathbb{R}^d$ . In this paper, we focus on low-dimensional signal generators with  $d = 2$  and high-dimensional dynamics with  $n$  up to 1000, a scale for which the use of traditional grid-based methods for PDEs is unpractical. Since the first-order system of nonlinear PDEs arising in the model reduction is similar to a system of Hamilton-Jacobi-Bellman PDEs from optimal feedback control, we

propose a numerical scheme based on Newton’s method in conjunction with a global polynomial ansatz for each PDE solution. This approach first explored in the context of Hamilton-Jacobi-Bellman PDEs in [8, 7] and later extended to high-dimensional settings in [23, 22, 6], mitigates the curse of dimensionality, scaling to large-scale systems at a moderate computational cost. The use of orthogonal polynomials for spectral and pseudospectral weighted residual methods for moment matching has been explored in [14] with linear signal generators and low-dimensional dynamics.

**1.1. Contribution.** This paper focuses on the development of computational methods for nonlinear moment matching. The main contributions are listed here:

- We develop and implement a Galerkin method to find approximate solutions to the invariance PDE system associated with the steady-state response of complex systems, and use these solutions to construct a reduced-order model to achieve moment matching.
- While many theoretical descriptions of reduced-order modeling by moment matching exist, there is a gap in the literature in developing computational methods for approximating the invariance equation for nonlinear moment matching. This paper represents the first attempt at explicitly developing a computational method to achieve these goals. In particular, the method’s ability to handle dynamics with thousands of states is an important novel contribution.
- The method’s efficacy is demonstrated in different complex examples, including systems of dimension up to 1000, systems where the nonlinearity is sinusoidal rather than polynomial in nature, and interconnected systems involving implicitly defined nonlinear signal generators.
- The method works in many different problems whenever the invariance PDE arises. In particular, this shows that the method is not only applicable to model order reduction problems, but also to other general control problems, for example output regulation, and immersion and invariance.

**1.2. Organization.** The paper is organized as follows. In [Section 2](#) we give an overview of the problem setup and we show how moment matching is defined and how the invariance PDE system arises. [Section 3](#) introduces a Galerkin type method for the numerical computation of an approximate solution  $\pi(\cdot)$  to the invariance PDE system. [Section 4](#) reports different numerical experiments assessing the accuracy of the proposed method and its effectiveness in generating a reduced-order model.

**2. Moment Matching for Nonlinear Dynamical Systems.** We consider dynamical systems with a state  $x(t) \in \mathbb{R}^n$  and an output  $y(t) \in \mathbb{R}^p$  of the form

$$(2.1) \quad \begin{aligned} \dot{x} &= f(x, u) \\ y &= h(x) \end{aligned}$$

where the input to the system is given by  $u(t) \in \mathbb{R}^m$ . We assume that the mappings  $f : \mathbb{R}^n \times \mathbb{R}^m \rightarrow \mathbb{R}^n$  and  $h : \mathbb{R}^n \rightarrow \mathbb{R}^p$  are  $C^r$  with  $r \geq 2$  and defined locally around the origin. Without loss of generality, we also assume that (2.1) has an equilibrium at the origin, that is,  $f(0, 0) = 0$  and  $h(0) = 0$ .

In order to introduce the notion of moment for a nonlinear system of the form (2.1), we consider the interconnection of (2.1) with an exogenous system, referred to as the *signal generator*, with a state  $\omega(t) \in \mathbb{R}^d$  which is described by equations of the

form

$$(2.2) \quad \begin{aligned} \dot{\omega} &= s(\omega), \\ v &= \ell(\omega), \end{aligned}$$

where  $v(t) \in \mathbb{R}^m$  is the output of the signal generator system, and the mappings  $s : \mathbb{R}^d \rightarrow \mathbb{R}^d$  and  $\ell : \mathbb{R}^d \rightarrow \mathbb{R}^m$  are  $C^r$  with  $r \geq 2$ . We also assume that (2.2) has an equilibrium at the origin.

Here, we introduce the notion of observability and accessibility, using the definitions introduced in [30], and based on [18] and [41]:

**DEFINITION 2.1 (Observability).** *The system (2.1) is said to be observable if for different initial conditions  $x_a(0) \neq x_b(0)$ , the output trajectories satisfy  $h(x_a(t)) \neq h(x_b(t))$  for some  $t \in \mathbb{R}$ , i.e. the output trajectories are not identical.*

**DEFINITION 2.2 (Accessibility).** *Let  $\mathcal{R}(x(0), T)$  be the set (reachable set) containing all points  $\bar{x}$  for which there exists an input  $u$  such that the evolution of (2.1) from  $x(0) \in \mathcal{X}$  satisfies  $x(t) \in \mathcal{X}$  for  $0 \leq t \leq T$  with  $x(T) = \bar{x}$ . The system (2.1) is said to be (locally) accessible if for all  $x(0) \in \mathcal{X}$  the set  $\bigcup_{t \leq T} \mathcal{R}(x(0), t)$  contains a non-empty open subset of  $\mathcal{X}$  for all  $T > 0$ .*

Throughout this article, we will assume that the system (2.1) is locally observable and locally accessible. We will also assume that the signal generator (2.2) is locally observable. From here, it is useful to establish definitions of Poisson stability and neutral stability of a system in connection to the signal generator.

**DEFINITION 2.3 (Poisson stability).** *A point  $\omega_0$  is said to be Poisson stable if, for each time  $T > 0$  and each neighbourhood  $U^0$  about  $\omega_0$ , the flow  $\omega^*(t)$  of  $s(\omega)$  with the initial condition  $\omega_0$  passes through  $U^0$  at points  $t_1 > T$  and  $t_2 < -T$ .*

**DEFINITION 2.4 (Neutral stability).** *A dynamical system is said to be neutrally stable if  $\omega = 0$  is a stable equilibrium, and there is an open neighbourhood  $W^0$  around the origin in which every point is Poisson stable.*

Clearly, if the signal generator is neutrally stable on a domain  $W^0$ , then  $\omega(t)$  is persistent in time and does not decay to zero as time tends towards infinity, for any initial condition  $\omega_0 \in W^0$ . Furthermore, this implies that the linear approximation of the system around the origin  $S = \left[ \frac{\partial s}{\partial \omega} \right] \Big|_{\omega=0}$  has purely imaginary eigenvalues, and that these eigenvalues are simple.

**2.1. Notion of Moment.** This paper focuses on the interconnected system (2.1)-(2.2) with the interconnection equation  $u = v$ . The interconnected system has a state-space representation given by

$$(2.3) \quad \begin{aligned} \dot{\omega}(t) &= s(\omega(t)), \\ \dot{x}(t) &= f(x(t), \ell(\omega(t))), \\ y(t) &= h(x(t)). \end{aligned}$$

The notion of the time-domain moment for a nonlinear dynamical system comes from analysing the steady-state output of the interconnected system given by (2.3) and makes use of the centre manifold theory. In order to help in our analysis of this interconnected dynamical system, we use the following definitions from [20] and [13].

**DEFINITION 2.5 (Centre Manifold, [13]).** *A mapping  $\pi$  between two coordinates  $\omega$  and  $x$  is an invariant manifold for a system of differential equations if the solution*

of the system given by  $(\omega(t), x(t))$  with initial condition  $(\omega_0, \pi(\omega_0))$ , lies on the curve  $(\omega(t), \pi(\omega(t)))$ .

Furthermore, if  $\pi(0) = 0$  and the tangent space  $\frac{\partial \pi}{\partial \omega}(0)$  is equal to the center subspace of the interconnected system, then it is also called a centre manifold. This subspace corresponds to exactly those eigenvalues of the interconnected system that have zero real part.

Under certain assumptions for the signal generator (2.2) and the system (2.1), we can assume that a locally attractive centre manifold exists between the two systems. We therefore make the following assumptions about the functions, based on [20]:

- (A1) The signal generator (2.2) is neutrally stable.
- (A2) The system (2.1) is asymptotically stable in the first approximation about the equilibrium at the origin. That is, the matrix  $A = \left[ \frac{\partial f}{\partial x} \right] \Big|_{\substack{x=0 \\ u=0}}$  has only eigenvalues with negative real part.

Based on these assumptions, we can conclude the following based on [20, Proposition 8.1.1].

**PROPOSITION 2.6.** *If Assumptions (A1) and (A2) hold, then we are guaranteed the existence of a mapping  $\pi : \mathbb{R}^d \rightarrow \mathbb{R}^n$  that is defined on a neighbourhood  $W^0$  about the origin and characterizes a locally attractive centre manifold for (2.3). This mapping  $\pi$  satisfies, for all  $\omega \in W^0$ ,*

$$(2.4) \quad \begin{aligned} \frac{\partial \pi}{\partial \omega} s(\omega) &= f(\pi(\omega), \ell(\omega)), \\ \pi(0) &= 0. \end{aligned}$$

*This centre manifold is represented as  $\mathcal{M} = \{(x, \omega) : x = \pi(\omega)\}$  for  $\pi$  solving (2.4). For each flow  $\omega^*(t)$  with  $\omega_0 \in W^0$  as an initial condition, the mapping  $\pi$  solving (2.4) produces a well-defined steady-state in the interconnected system  $y_{ss}(t) = h(\pi(\omega^*(t)))$ .*

Note that in the case where the system (2.1) and the signal generator (2.2) are both linear, with  $s(\omega) = S\omega$ ,  $\ell(\omega) = L\omega$  and  $f(x, u) = Ax + Bu$ , the invariance equation (2.4) simplifies to the well-known Sylvester equation

$$(2.5) \quad \Pi S = A\Pi + BL$$

where the matrix  $\Pi$  represents the invariant mapping  $x = \Pi\omega$ .

If the initial condition of the signal generator satisfies  $\omega_0 \in W^0$  and if the initial condition  $x_0$  of the system is sufficiently close to the centre manifold, then the centre manifold is said to be locally attractive if we have

$$(2.6) \quad \|x(t) - \pi(\omega^*(t))\| \leq Ke^{-\alpha t} \|x_0 - \pi(\omega_0)\|, \quad \text{for some } K \geq 1, \alpha > 0.$$

This implies that

$$(2.7) \quad \lim_{t \rightarrow \infty} \|y(t) - h(\pi(\omega^*(t)))\| = 0.$$

The steady-state response of the system is therefore defined by the invariant mapping between  $\omega$  and  $x$ , which allows us to define what we mean by a system's moment.

DEFINITION 2.7 (Moment). *Assume that (2.4) has a solution  $\pi$  for the interconnected system (2.3). Then the time-domain moment of the interconnected system at  $(s, \ell)$  is given by the function  $h(\pi(\omega(\cdot)))$ .*

Assumptions (A1) and (A2) guarantee that (2.4) has a solution, and that the notion of moment is in one-to-one relation with the steady-state response of output of the interconnected system (2.3) for initial conditions starting near the centre manifold  $\mathcal{M}$ . In the rest of the paper, we shall assume that assumptions (A1) and (A2) hold.

Note that in the linear case, if  $f$  has a locally asymptotically stable equilibrium, then it is also globally asymptotically stable. Thus, the transient response due to any initial condition  $x_0$  will disappear, and we can say that the invariant manifold is globally attractive.

**2.2. Moment-Based Reduced-Order Modeling.** With the help of our previously defined notion of moment, we would like to use moment matching to develop a reduced-order model that is able to predict the long-term behaviour of the interconnected system, given a known signal generator input. The reduced-order model takes the form

$$(2.8) \quad \begin{aligned} \dot{r}(t) &= \bar{f}(r(t), u(t)) \\ y_r(t) &= \bar{h}(r(t)) \end{aligned}$$

with  $r(t) \in \mathbb{R}^v$ , with  $v \ll n$ ,  $u(t) \in \mathbb{R}^m$ ,  $\bar{f}$  is a  $C^r$  mapping  $\bar{f} : \mathbb{R}^v \times \mathbb{R}^m \rightarrow \mathbb{R}^v$  satisfying  $\bar{f}(0, 0) = 0$ . The output  $y_r(t) \in \mathbb{R}^p$  is measured by the  $C^r$  mapping  $\bar{h} : \mathbb{R}^v \rightarrow \mathbb{R}^p$ .

Reduced-order modeling by moment matching involves constructing a system where the observed output  $y_r(t)$  is in some sense similar to the output of the system  $y(t)$  when the input to each system is given by the signal generator. In particular, we are interested in constructing systems where the dimension of the reduced-order model is much smaller,  $v \ll n$ . The main objective behind this is to create smaller models that preserve the behaviour of the system when subjected to signals of interest.

We will use the following definition of a reduced-order model based on [3]:

DEFINITION 2.8. *The system described by (2.8) is a model at  $s(\omega)$  of the system (2.1) if it has the same moment at  $s(\omega)$  as (2.1). In this case, it is said to match the moment of the system at  $s(\omega)$ . Furthermore, system (2.8) is a reduced-order model of system (2.1) if  $v < n$ .*

If the reduced-order model satisfies assumption (A2), then we know that there exists a mapping  $p(\cdot)$  satisfying the equation

$$(2.9) \quad \begin{aligned} \frac{\partial p}{\partial \omega} s(\omega) &= \bar{f}(p(\omega), \ell(\omega)) \\ p(0) &= 0. \end{aligned}$$

Under these assumptions, the steady-state output of (2.8) is given by

$$(2.10) \quad \lim_{t \rightarrow \infty} |y_r(t) - \bar{h}(p(\omega(t)))| = 0.$$

Therefore, the reduced-order model (2.8) matches the moments of the (2.1) at  $s(\omega)$  if the mapping that solves (2.9) also satisfies

$$(2.11) \quad h(\pi(\omega)) = \bar{h}(p(\omega)).$$

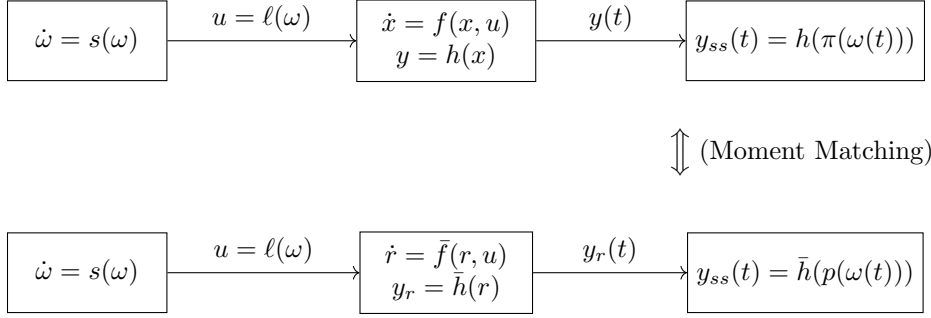


Fig. 1: Diagrammatic illustration of the concepts of moment matching in reduced-order modeling. The signal generator generates a control input to the higher order model and the reduced-order model, and moment-matching corresponds to the exact matching of their steady-state responses.

Figure 1 depicts how moment matching corresponds to the matching of the steady-state responses of the full-order model and reduced-order model.

In order to construct a reduced-order model, we need to choose mappings  $\bar{f}$  and  $\bar{h}$  such that the equilibrium  $(0,0)$  of  $\bar{f}$  is locally exponentially stable in the first approximation, and such that (2.9) and (2.11) hold. We note that choosing  $p(\omega) = \omega$  and  $\bar{h}(\omega) = h(\pi(\omega))$  allows the reduced-order model to satisfy (2.11), and as a consequence simplifies (2.9) to

$$(2.12) \quad s(\omega) = \bar{f}(\omega, \ell(\omega)).$$

In particular, the choice of  $p(\omega) = \omega$  gives us a family of reduced-order models

$$(2.13) \quad \begin{aligned} \dot{r} &= s(r) - \bar{g}(r, \ell(r)) + \bar{g}(r, u) \\ y_r &= \bar{h}(\pi(r)) \end{aligned}$$

where the mapping  $\bar{g}$  is a free parameter, which can be chosen to ensure the local asymptotic stability about the origin of the autonomous system having vector field

$$(2.14) \quad s(r) - \bar{g}(r, \ell(r)).$$

A suitable choice of  $\bar{g}$  can therefore ensure that Assumption (A2) holds, and that the reduced-order model given by (2.13) achieves moment matching.

It is convenient to have  $\bar{g}$  take the form  $\bar{g}(r, \ell(r)) = g(r)\ell(r)$  for some  $C^r$  mapping  $g: \mathbb{R}^d \rightarrow \mathbb{R}^{d \times m}$ . In the general case, one suitable mapping can be found by computing

$$(2.15) \quad S = \left[ \frac{\partial s(r)}{\partial r} \right] \Big|_{(r=0)}, \quad L = \left[ \frac{\partial \ell(r)}{\partial r} \right] \Big|_{(r=0)}$$

and choosing a mapping  $g(r) = G$  for some real-valued matrix  $G$  satisfying that  $S - GL$  has only eigenvalues with negative real part, which can be accomplished if  $(S, L)$  is detectable. The linearization of (2.14) then simply becomes  $S - GL$ , and the assumption on the eigenvalues of  $S - GL$  ensures that the system is therefore locally exponentially stable.

**3. Approximate solutions via Galerkin expansion.** The main difficulty in constructing a reduced-order model by moment matching lies in obtaining a suitable mapping  $\pi(\cdot)$  satisfying the PDE system

$$(3.1) \quad \begin{aligned} \frac{\partial \pi}{\partial \omega} s(\omega) &= f(\pi(\omega), \ell(\omega)), \\ \pi(0) &= 0. \end{aligned}$$

This is in general, a difficult problem to solve, as we have to solve a potentially large-scale, high-dimensional system of coupled nonlinear PDEs. A method of approximating the solution to the PDE system (3.1) is proposed in this section.

**3.1. Polynomial expansion of the invariant mapping.** Proposition 2.6 only guarantees the existence of a solution to system (3.1) in a neighbourhood of the origin, hence we restrict our analysis to a domain  $\Omega \subset \mathbb{R}^d$  containing the origin. We denote the  $i$ -th row of the  $n$ -dimensional mapping  $\pi$  as  $\pi_i$ , so  $\pi(\omega) = (\pi_1(\omega), \pi_2(\omega), \dots, \pi_n(\omega))^\top$ . For each mapping  $\pi_i : \mathbb{R}^d \rightarrow \mathbb{R}$ ,  $i = 1, \dots, n$ , we consider an expansion  $\pi_i^N$  of the form

$$(3.2) \quad \pi_i^N(\omega) = \sum_{k=1}^N c_{i,k} \phi_k(\omega) = \Phi^N \mathbf{c}_i$$

where  $\Phi^N = (\phi_1, \phi_2, \dots, \phi_N)$ , and where  $\{\phi_k\}_{k=1, \dots, N}$  satisfy  $\phi_k \in C^\infty(\Omega)$  and belong to a complete family of basis functions in  $L^2(\Omega)$ . For this problem, we are interested in globally supported ansatz functions, such as monomials or orthogonal polynomials. The Galerkin residual method finds a weak solution to the invariant manifold  $\pi$  by projecting the mapping onto the space of functions  $\{\phi_k\}$  and ensuring that the approximation error of the equation is orthogonal to every  $\phi_j$  in the basis. The method of weighted residuals presented here, and the resulting residual equations shown later, are similar to those presented in [14] and [23].

The coefficients of  $c_i$  in (3.2) for  $i = 1, \dots, n$  are found by setting the projection of the error in (3.1) to zero for all  $x \in \Omega$  and imposing the Galerkin residual equation

$$(3.3) \quad \left\langle \frac{\partial \pi_i}{\partial \omega} s - f_i(\pi(\omega), \ell(\omega)), \phi_j \right\rangle_\Omega = 0, \quad \forall \phi_j \in \Phi^N$$

where the inner product is defined as

$$(3.4) \quad \langle f, g \rangle_\Omega = \int_\Omega f(\omega) g(\omega) d\omega.$$

For the sake of simplicity, based on the notation used in [7], with a slight abuse of notation we define the following extension of the inner product for vector-valued functions:

DEFINITION 3.1. *If  $\eta : \mathbb{R}^N \rightarrow \mathbb{R}$  is a real-valued function, then we define*

$$(3.5) \quad \langle \eta, \Phi^N \rangle_\Omega = (\langle \eta, \phi_1 \rangle_\Omega, \dots, \langle \eta, \phi_N \rangle_\Omega)^\top.$$

*If  $\eta : \mathbb{R}^N \rightarrow \mathbb{R}^N$  is a real-valued function, then we define*

$$(3.6) \quad \langle \eta, \Phi^N \rangle_\Omega = \begin{bmatrix} \langle \eta_1, \phi_1 \rangle_\Omega & \dots & \langle \eta_N, \phi_1 \rangle_\Omega \\ \vdots & & \vdots \\ \langle \eta_1, \phi_N \rangle_\Omega & \dots & \langle \eta_N, \phi_N \rangle_\Omega \end{bmatrix}.$$



In order to solve the nonlinear system (3.3), we introduce the high-dimensional function  $F(\cdot) : \mathbb{R}^{Nn} \rightarrow \mathbb{R}^{Nn}$ ,

$$(3.7) \quad F(\mathbf{c}) := (F_1(\mathbf{c}), \dots, F_i(\mathbf{c}), \dots, F_n(\mathbf{c}))^\top$$

where each  $F_i$  is itself a multi-dimensional function  $F_i : \mathbb{R}^{Nn} \rightarrow \mathbb{R}^N$ , given by

$$(3.8) \quad F_i(\mathbf{c}) = \begin{bmatrix} \left\langle \frac{\partial \pi_i^N}{\partial \omega} s(\omega) - f_i(\pi^N(\omega), \ell(\omega)), \phi_1 \right\rangle_\Omega \\ \vdots \\ \left\langle \frac{\partial \pi_i^N}{\partial \omega} s(\omega) - f_i(\pi^N(\omega), \ell(\omega)), \phi_N \right\rangle_\Omega \end{bmatrix}.$$

By expanding  $\pi^N$  in this function, we express each  $F_i$  as a sum of linear and nonlinear components on  $\mathbf{c}_i$ . Using our notation for inner products, we can represent each  $F_i(\cdot)$  as

$$(3.9) \quad F_i(\mathbf{c}) = \left\langle \frac{\partial \Phi^N}{\partial \omega} \cdot s, \Phi^N \right\rangle_\Omega \mathbf{c}_i - \left\langle f_i \left( [\Phi^N \mathbf{c}_1, \dots, \Phi^N \mathbf{c}_n]^\top, \ell(\omega) \right), \Phi^N \right\rangle_\Omega.$$

The linear term can be written as a matrix-vector product  $\mathbf{A}\mathbf{c}$ , where  $\mathbf{A}$  is defined as

$$(3.10) \quad \mathbf{A} = \left\langle \frac{\partial \Phi^N}{\partial \omega} \cdot s, \Phi^N \right\rangle_\Omega.$$

In order to deal with the second term in the right hand side of the expression, for convenience, we can define the function  $G : \mathbb{R}^{Nn} \rightarrow \mathbb{R}^{Nn}$  as  $G(\mathbf{c}) = (G_1(\mathbf{c}), \dots, G_n(\mathbf{c}))^\top$  with

$$(3.11) \quad G_i(\mathbf{c}) = - \left\langle f_i \left( [\Phi^N \mathbf{c}_1, \dots, \Phi^N \mathbf{c}_n]^\top, \ell(\omega) \right), \Phi^N \right\rangle_\Omega.$$

Using this notation, we can then write  $F_i$  as

$$(3.12) \quad F_i(\mathbf{c}) = \mathbf{A}\mathbf{c}_i + G_i(\mathbf{c})$$

and the overall function as

$$(3.13) \quad F(\mathbf{c}) = \mathbf{A} \begin{bmatrix} \mathbf{c}_1 \\ \vdots \\ \mathbf{c}_n \end{bmatrix} + G(\mathbf{c}).$$

*Remark 3.2.* If the function  $f$  determining the system's dynamics is polynomial and sufficiently low-dimensional, for example if it is linear, quadratic, or cubic in  $\pi$ , the functions  $G_i$  can be represented with matrices and tensors similar to  $\mathbf{A}$ . In problems where this is the case, it will be useful to construct a matrix or tensor representation of the function in order to accelerate both assembly and iterative computations.

In order to find the coefficients  $\mathbf{c}$  satisfying  $F(\mathbf{c}) = 0$ , we employ a Newton iteration, which iterates until  $|F(\mathbf{c})|_1$  is below a given tolerance. To carry out this iteration, we also need to find the Jacobian of the Galerkin residual function. The

Jacobian is defined as  $JF : \mathbb{R}^{Nn} \rightarrow \mathbb{R}^{Nn} \times \mathbb{R}^{Nn}$ , with  $JF(\mathbf{c}) = \frac{\partial F}{\partial \mathbf{c}}(\mathbf{c})$ . Based on our formulation in (3.9), we represent it as

$$(3.14) \quad JF(\mathbf{c}) = \begin{bmatrix} JF_{1,1}(\mathbf{c}) & \dots & JF_{n,1}(\mathbf{c}) \\ \vdots & & \vdots \\ JF_{1,n}(\mathbf{c}) & \dots & JF_{n,n}(\mathbf{c}) \end{bmatrix}$$

where the corresponding entries are given by

$$(3.15) \quad JF_{i,j}(\mathbf{c}) = \delta_{ij}\mathbf{A} + \frac{\partial G_i}{\partial \mathbf{c}_j}(\mathbf{c}).$$

Here,  $\delta_{ij}$  denotes the Kronecker delta acting on the indices  $i$  and  $j$ . The functions  $\frac{\partial G_i}{\partial \mathbf{c}_j}$  can be computed using the chain rule:

$$(3.16) \quad \frac{\partial G_i}{\partial \mathbf{c}_j}(\mathbf{c}) = - \left\langle \frac{\partial f_i(\pi^N(\omega), \ell(\omega))}{\partial \mathbf{c}_j} \Phi^N, \Phi^N \right\rangle_{\Omega} \Big|_{\pi = \Phi^N \mathbf{c}}.$$

Based on the expression of  $F(\mathbf{c})$  in (3.9) and of  $JF(\mathbf{c})$  in (3.15), the Newton update reads

$$(3.17) \quad \mathbf{c}^{k+1} = \mathbf{c}^k - JF(\mathbf{c}^k)^{-1}F(\mathbf{c}^k)$$

*Remark 3.3.* Note that in some cases, depending on the system dynamics under study, the Jacobian  $JF$  may become singular. In these scenarios, we replace the inverse Jacobian  $JF^{-1}$  with the Moore-Penrose inverse (pseudoinverse). However, since the Jacobian is not full-rank, the convergence of the algorithm to the appropriate approximation  $\pi^N$  will then depend on having a good initialization for the coefficients  $\mathbf{c}^0$ .

**3.2. Polynomial basis.** The construction of the polynomial basis for our approximation largely follows the procedure used in [23, Section 4.1]. In order to construct the basis functions to be used in the Galerkin approximation over the  $d$ -dimensional space  $\Omega$ , we must first select a maximum degree  $M$  and a one-dimensional basis  $\varphi_M : \mathbb{R} \rightarrow \mathbb{R}^M$ . In our case, we will use the monomial basis

$$(3.18) \quad \varphi(\omega) = (\omega, \omega^2, \dots, \omega^M).$$

Note that, since our invariance equation (3.1) specified that  $\pi(0) = 0$ , we do not require a constant term in our basis. In this paper we are using a monomial basis but in general, it is possible to use the same generation method based on a different chosen one-dimensional basis, for example orthogonal bases such as Legendre or Chebyshev polynomials up to degree  $M$ .

In order to generate the multi-dimensional basis, we use the tensor product of the one-dimensional basis and eliminate those terms whose total degree is higher than the prescribed maximum degree  $M$ . The basis is then given by

$$(3.19) \quad \Phi^N = \left\{ \phi \in \bigotimes_{j=1}^d \varphi(\omega_j), \text{ where } \text{deg}(\phi) \leq M \right\}.$$

The number of basis functions  $N$  is related combinatorially to the maximum degree  $M$ , as

$$(3.20) \quad N = \sum_{m=1}^M \binom{d+m-1}{m} = \frac{M+1}{d} \binom{M+d}{M+1} - 1.$$

In our case, where the one-dimensional basis is just given as the monomials up to degree  $M$ , each basis polynomial  $\phi_i$  can be conveniently written as the separable function

$$(3.21) \quad \phi_i = \prod_{j=1}^d \phi_i^j(x_j) = \prod_{j=1}^d \omega_j^{\nu_{i,j}} \text{ where } \sum_{j=1}^d \nu_{i,j} \leq M$$

for coefficients  $\nu_{i,j}$ .

**3.3. Integration.** We are concerned with the assembly of  $\mathbf{A}$ ,  $G_i$ , and  $\frac{\partial G_i}{\partial \mathbf{c}_j}$

1.  $\mathbf{A} = \left\langle \frac{\partial \Phi^N}{\partial \omega} \cdot s, \Phi^N \right\rangle_{\Omega}$ : Each component of this matrix is computed using the calculation

$$(3.22) \quad \mathbf{A}_{i,j} = \left\langle \frac{\partial \phi_j}{\partial \omega} \cdot s, \phi_i \right\rangle_{\Omega} = \sum_{k=1}^d \int_{\Omega} \frac{d\phi_j(\omega)}{d\omega_k} s_k(\omega) \phi_i(\omega) d\omega,$$

where  $s(\omega) = (s_1(\omega), \dots, s_d(\omega))^{\top}$ . Depending on the expansion of each  $s_k(\omega)$ , for example if they are monomials, this expression can be computed exactly.

2.  $G_i(\mathbf{c}) = -\langle f_i(\pi^N(\omega), \ell(\omega)), \Phi^N \rangle_{\Omega}$ : Each component of the vector function  $G$  is represented as

$$(3.23) \quad G_i(\mathbf{c})_j = -\langle f_i(\pi^N(\omega), \ell(\omega)), \phi_j \rangle_{\Omega} = -\int_{\Omega} f_i(\pi^N(\omega), \ell(\omega)) \phi_j(\omega) d\omega.$$

The evaluation of these integrals for  $i = 1, \dots, n$  can be approximated using a suitable quadrature rule, for example the Gauss-Legendre quadrature in  $d$  dimensions over the domain  $\Omega$ , up to a desired accuracy.

3.  $\frac{\partial G_i}{\partial \mathbf{c}_j} = -\left\langle \frac{\partial f_i(\pi^N(\omega), \ell(\omega))}{\partial \mathbf{c}_j} \Phi^N, \Phi^N \right\rangle_{\Omega}$ : We proceed similarly as for  $G_i(\mathbf{c})$ . We have the expression

$$(3.24) \quad \begin{aligned} \frac{\partial G_i}{\partial \mathbf{c}_j}_{k,l} &= -\left\langle \frac{\partial f_i(\pi^N(\omega), \ell(\omega))}{\partial \mathbf{c}_j} \phi_l \phi_k \right\rangle_{\Omega} \\ &= -\int_{\Omega} \frac{\partial f_i(\pi^N(\omega), \ell(\omega))}{\partial \mathbf{c}_j} \phi_l(\omega) \phi_k(\omega) d\omega. \end{aligned}$$

This integral is approximated by a suitable quadrature rule.

**3.4. Computational complexity and implementation.** The bulk of the computation comes from integration over  $d$  dimensions, as well as the inversion of the matrix  $JF$ . The computational complexity of integration over  $d$  dimensions scales exponentially with  $d$ , meaning that if the nonlinearities in  $f$  do not allow a convenient matrix or tensor representation of  $G_i$  as discussed in Remark 3.2, then we encounter the curse of dimensionality in computing the integral when  $d$  becomes large.

The inversion of the Jacobian matrix scales approximately cubically with the size of the matrix,  $Nn$ . This is therefore dependent on the size of the system,  $n$ , and is

indirectly combinatorially dependent on the dimensionality  $d$  of the signal generator and the maximum degree  $M$ . Part of the objective of our polynomial approximation is therefore to find an appropriate, relatively low, maximum degree  $M$  where  $\pi^N$  sufficiently approximates the solution to (3.1), and to see how the approximation error scales with the maximum degree.

**3.5. Evaluating approximate solutions.** The approximate solution  $\pi^N(\omega)$  can be verified by analyzing the residual of the equation (3.1). In essence, we are measuring the residual error of  $n$  different PDEs, and so we can define the residual error function as

$$(3.25) \quad R(\mathbf{c}, \omega) = (R_1(\mathbf{c}, \omega), \dots, R_n(\mathbf{c}, \omega))^\top,$$

where for each dimension  $i = 1, \dots, n$  the residual at a specified  $\omega$  is given by

$$(3.26) \quad R_i(\mathbf{c}, \omega) = \frac{\partial \pi_i^N}{\partial \omega} s(\omega) - f(\pi^N(\omega), \ell(\omega)).$$

In order to quantify how well a given set of coefficients  $\mathbf{c}$  approximates the solution, we compute the  $L_2$  norm of each  $R_i$ , averaged over a chosen subdomain  $W \subseteq \Omega$ , as

$$(3.27) \quad \|R_i\|_{(2,W)} = \sqrt{\int_W |R_i(\mathbf{c}, \omega)|^2 d\omega}.$$

Finally, to generate a single metric measuring the success of the approximation, we consider the average over all  $i = 1, \dots, n$  of  $\|R_i\|_{(2,W)}$ , weighted by the relative magnitude of the coefficients  $\mathbf{c}_i$ :

$$(3.28) \quad \|R\|_{(2,W)} = \frac{\sum_{i=1}^n \|\mathbf{c}_i\|_2 \|R_i\|_{(2,W)}}{\sum_{i=1}^n \|\mathbf{c}_i\|_2}.$$

**4. Numerical results.** Different numerical tests were performed to assess the domain over which a good approximation could be found with a relatively low maximum degree in the Galerkin expansion, due to the increasing computational complexity of the problem with higher dimensional expansions. These tests were carried out over chosen rectangular domains  $\Omega$  of varying sizes, for different nonlinear dynamics and signal generators, and the algorithm was employed with a tolerance of  $10^{-7}$  in the  $L^1$  norm of  $F$ . Two Python modules for solving the invariance PDE and for generating the reduced-order model, as well as several scripts to replicate the results shown in this section, can be found at <https://github.com/carlosjdoebeli/Moment-Matching-ROM>.

**4.1. Summary of examples.** We primarily looked at four different examples to test our method and its limitations. The first two examples serve as a proof-of-concept for the method and shows its ability to recover known analytical solutions from low-dimensional nonlinear systems. The first two tests, outlined in Subsection 4.2 and Subsection 4.3, are nonlinear, and demonstrate the algorithm's ability to recover highly accurate solutions when the components of  $\pi$  belong to the span of the basis.

The third and fourth examples, in Subsection 4.4 and Subsection 4.5, show the method's ability to recover solutions for larger nonlinear systems with both a linear

and nonlinear signal generator. Tests are done with a full-order model dimensionality of  $n = 2$ ,  $n = 100$ , and  $n = 1000$ , to demonstrate the scalability of the method to large nonlinear systems. Because the analytical solution is not known, we test the reduced-order model's ability to recreate the signal produced by the full-order model in these cases, alongside evaluating the residual error.

**4.2. Test 1: Low-dimensional nonlinear system.** First, we consider the model presented in [20, Example 8.1.3] with  $n = 2, d = 2$  given by

$$\begin{aligned} s(\omega) &= a \begin{bmatrix} \omega_2 \\ -\omega_1 \end{bmatrix} & \ell(\omega) &= \omega_1 \\ f(x, u) &= \begin{bmatrix} -x_1 + u \\ -x_2 + x_1 u \end{bmatrix} & h(x) &= x_1. \end{aligned}$$

For this problem, the map  $\pi$  admits the analytical solution

$$\pi(\omega_1, \omega_2) = \left( \frac{1}{1+a^2}(\omega_1 - a\omega_2), \frac{1}{1+5a^2+4a^4}((1+a^2)\omega_1^2 - 3a\omega_1\omega_2 + 3a^2\omega_2^2) \right)^\top.$$

Note that the answer can be expressed in monomials in  $\omega$  up to degree two, which lies in the span of our chosen basis.

Using our representations of  $G_i$  in (3.23) and  $\frac{\partial G_i}{\partial \mathbf{c}_j}$  in (3.24), we can compute the function  $F$  and its Jacobian as

$$F(\mathbf{c}) = \begin{bmatrix} \mathbf{A}\mathbf{c}_1 + \mathbf{M}\mathbf{c}_1 - \boldsymbol{\gamma} \\ \mathbf{A}\mathbf{c}_2 + \mathbf{M}\mathbf{c}_2 - \mathbf{P}\mathbf{c}_1 \end{bmatrix}, \quad JF(\mathbf{c}) = \begin{bmatrix} \mathbf{A} + \mathbf{M} & 0 \\ -\mathbf{P} & \mathbf{A} + \mathbf{M} \end{bmatrix}$$

using the previously defined matrix  $\mathbf{A}$  in (3.22), as well as defining

$$(4.1) \quad \mathbf{M} = \langle \Phi^N, \Phi^N \rangle_\Omega, \quad \mathbf{P} = \langle \Phi^N \omega_1, \Phi^N \rangle_\Omega, \quad \boldsymbol{\gamma} = \langle \ell(\omega), \Phi^N \rangle_\Omega.$$

Using a constant  $a = 2$  and a domain of  $\Omega = [-1, 1]^2$ , the Galerkin method attains nearly exact recovery of the analytical solution, as shown in Table 1.

Domain	$M = 2$	$M = 4$	$M = 6$
$\Omega = [-1, 1]^2$	$1.1048 \times 10^{-16}$	$1.0940 \times 10^{-15}$	$5.7176 \times 10^{-14}$

Table 1: Table of the average residual error  $\|R(\mathbf{c}, \omega)\|_{(2, W)}$  for the Galerkin approximation of the invariant mapping  $\pi$  for Test 1 with a constant  $a = 2$ . The error is shown for different values of  $M$  over the domain  $W = [-1, 1]^2$ .

**4.3. Test 2: Cart pendulum.** We also consider the position control of a nonlinear cart pendulum, based on a problem studied in [32, Section 3.2]. The signal generator is chosen by selecting target dynamics for the cart pendulum with  $d = 2$  and  $n = 4$ . The dynamics of the interconnected system are then governed by the equations

$$s(\omega) = \begin{bmatrix} \omega_2 \\ \frac{a_1 \sin(\omega_1)}{1 + k a_2 \cos(\omega_1)} \end{bmatrix}, \quad \ell(\omega) = \frac{k a_1 \sin(\omega_1)}{1 + k a_2 \cos(\omega_1)}, \quad k < -\frac{1}{a_2}$$

$$f(x, u) = \begin{bmatrix} x_3 \\ x_4 \\ a_1 \sin(x_1) - a_2 \cos(x_1)u \\ u \end{bmatrix}, \quad h(x) = x_1 \quad a_1 > 0, a_2 > 0.$$

This problem is known to admit an analytical solution given as

$$\pi(\omega) = (\omega_1, k\omega_1, \omega_2, k\omega_2)^\top.$$

With respect to our algorithm,  $F$  and  $JF$  are represented as

$$F(\mathbf{c}) = \begin{bmatrix} \mathbf{A}\mathbf{c}_1 - \mathbf{M}\mathbf{c}_3 \\ \mathbf{A}\mathbf{c}_2 - \mathbf{M}\mathbf{c}_4 \\ \mathbf{A}\mathbf{c}_3 - H(\mathbf{c}_1) \\ \mathbf{A}\mathbf{c}_4 - \boldsymbol{\beta} \end{bmatrix}, \quad JF(\mathbf{c}) = \begin{bmatrix} \mathbf{A} & 0 & -\mathbf{M} & 0 \\ 0 & \mathbf{A} & 0 & -\mathbf{M} \\ -\frac{\partial H}{\partial \mathbf{c}_1} & 0 & \mathbf{A} & 0 \\ 0 & 0 & 0 & \mathbf{A} \end{bmatrix}$$

where  $\mathbf{A}$ ,  $\mathbf{M}$  and  $\boldsymbol{\gamma}$  are defined as before in (3.22), and (4.1), and the function  $H : \mathbb{R}^N \rightarrow \mathbb{R}^N$  is given by

$$\begin{aligned} H(\mathbf{c}_1) &= \langle a_1 \sin(\Phi^N \mathbf{c}_1) - a_2 \cos(\Phi^N \mathbf{c}_1) \ell(\omega), \Phi^N \rangle_\Omega \\ \frac{\partial H}{\partial \mathbf{c}_1} &= \langle \Phi^N (a_1 \cos(\Phi^N \mathbf{c}_1) + a_2 \sin(\Phi^N \mathbf{c}_1) \ell(\omega)), \Phi^N \rangle_\Omega. \end{aligned}$$

In this problem, due to the choice of  $s(\omega)$ , the matrix  $A$  is singular, and therefore the Jacobian  $JF$  is also singular. Therefore, we must use the pseudoinverse to solve for our optimal  $\pi^N$ . We must then be careful in selecting our starting guess for  $\mathbf{c}^0$ ; since the analytical solution contains coefficients that are mostly zero, we choose a starting guess of constants that are uniformly zero.

Using the constants  $a_1 = 2$ ,  $a_2 = 3$ , and  $k = -\frac{2}{3}$ , and a starting guess of  $\mathbf{c} = 0$ , the Galerkin method is able to recover the analytical solution. Table 2 once again shows a negligible error in the solution, close to machine precision, and reducing the tolerance yields even smaller errors. Note that in both this and the previous example, the solution admitted a monomial representation and the algorithm was able to achieve exact recovery.

Domain	$M = 2$	$M = 4$	$M = 6$
$\Omega = [-1, 1]^2$	$9.3256 \times 10^{-10}$	$8.6338 \times 10^{-10}$	$9.4227 \times 10^{-10}$

Table 2: Table of the average error  $\|R(\mathbf{c}, \omega)\|_{(2, W)}$  for the Galerkin approximation of the invariant mapping  $\pi$  for Test 2 with a constants  $a_1 = 2, a_2 = 3, k = -\frac{2}{3}$ . The error is shown for the domains  $\Omega = [-1, 1]^2$ , as well as for different maximal degrees of  $m = 3, m = 4$ , and  $m = 6$ .

**4.4. Test 3: Nonlinear resistor-inductor ladder with linear oscillator as signal generator.** We consider the nonlinear resistor-inductor (RL) ladder, based on a slightly modified version of the schematic in [34, Figure 7] and also appearing in a similar context for model order reduction in [24]. The signal generator has dimension  $d = 2$ , and the system has a repeating structure that allows for considering any

number of dimensions  $n$ . This experiment is particularly interesting because there is no analytical solution, and it will allow us to determine whether our method is able to find a good approximate solution. The signal generator is given by:

$$(4.2) \quad s(\omega) = \begin{bmatrix} 0 & a \\ -a & 0 \end{bmatrix} \begin{bmatrix} \omega_1 \\ \omega_2 \end{bmatrix}, \quad \ell(\omega) = \omega_2, \quad a \in \mathbb{R} \setminus \{0\}$$

and the system satisfies

$$(4.3) \quad \begin{bmatrix} \dot{x}_1 \\ \dot{x}_2 \\ \vdots \\ \dot{x}_{n-1} \\ \dot{x}_n \end{bmatrix} = \underbrace{\begin{bmatrix} -2\kappa & 1 & & & \\ 1 & -2\kappa & 1 & & \\ & \ddots & \ddots & \ddots & \\ & & & 1 & -2\kappa & 1 \\ & & & & 1 & -2\kappa \end{bmatrix} \begin{bmatrix} x_1 \\ x_2 \\ \vdots \\ x_{n-1} \\ x_n \end{bmatrix} - \begin{bmatrix} x_1^2/2 + x_1^3/3 \\ x_2^2/2 + x_2^3/3 \\ \vdots \\ x_{n-1}^2/2 + x_{n-1}^3/3 \\ x_n^2/2 + x_n^3/3 \end{bmatrix} + \begin{bmatrix} 1 \\ 0 \\ \vdots \\ 0 \\ 0 \end{bmatrix} u}_{=: f(x, u)}$$

$$h(x) = x_1.$$

The dynamics above depend on a parameter  $\kappa$ . Using  $\kappa = 1$ , the system no longer satisfies the necessary assumptions above a certain number of degrees  $n$ , and becomes unstable, so we use a value of  $\kappa$  close to 1 but slightly bigger than 1. Since the nonlinearities in each  $f_i$  are polynomials of degree 2 and 3 and only depend on the corresponding  $x_i$ , we can make the following simplifications in the construction of  $F$  and  $JF$ .

We begin by defining the tensors  $\mathbf{N}$  and  $\mathbf{O}$ :

$$(4.4) \quad \begin{aligned} \mathbf{N} &\in \mathbb{R}^{N^3}, [\mathbf{N}]_{i,j,k} = \int_{\Omega} \phi_i \phi_j \phi_k d\omega \\ \mathbf{O} &\in \mathbb{R}^{N^4}, [\mathbf{O}]_{i,j,k,l} = \int_{\Omega} \phi_i \phi_j \phi_k \phi_l d\omega. \end{aligned}$$

We now also introduce the functions  $\tilde{N} : \mathbb{R}^N \rightarrow \mathbb{R}^{N \times N}$  and  $\tilde{O} : \mathbb{R}^N \rightarrow \mathbb{R}^{N \times N}$ , intended to act upon each  $\mathbf{c}_i$ . They are defined by

$$(4.5) \quad [\tilde{N}(\mathbf{v})]_{i,j} = \sum_{k=1}^N v_k N_{i,j,k}, \quad [\tilde{O}(\mathbf{v})]_{i,j} = \sum_{k=1}^N \sum_{l=1}^N v_k v_l O_{i,j,k,l}.$$

Finally, define the functions  $P, Q : \mathbb{R}^N \rightarrow \mathbb{R}^{N \times N}$  as

$$(4.6) \quad \begin{aligned} P(\mathbf{v}) &= \left( \mathbf{A} + 2\kappa \mathbf{M} + \frac{1}{2} \tilde{N}(\mathbf{v}) + \frac{1}{3} \tilde{O}(\mathbf{v}) \right) \mathbf{v} \\ Q(\mathbf{v}) &= \mathbf{A} + 2\kappa \mathbf{M} + \tilde{N}(\mathbf{v}) + \tilde{O}(\mathbf{v}), \end{aligned}$$

where  $\mathbf{A}$  and  $\mathbf{M}$  are as given in (3.22) and (4.1).

Then the function  $F$  is represented in each dimension as

$$(4.7) \quad F_i(\mathbf{c}) = P(\mathbf{c}_i) - (1 - \delta_{i,1}) \mathbf{M} \mathbf{c}_{i-1} - (1 - \delta_{i,n}) \mathbf{M} \mathbf{c}_{i+1} - \delta_{i,1} \boldsymbol{\gamma},$$

where  $\boldsymbol{\gamma}$  is the same as in (4.1), and its Jacobian is given by

$$(4.8) \quad JF(\mathbf{c}) = \begin{bmatrix} Q(\mathbf{c}_1) & -\mathbf{M} & & & & \\ -\mathbf{M} & Q(\mathbf{c}_2) & -\mathbf{M} & & & \\ & \ddots & \ddots & \ddots & & \\ & & & -\mathbf{M} & Q(\mathbf{c}_{n-1}) & -\mathbf{M} \\ & & & & -\mathbf{M} & Q(\mathbf{c}_n) \end{bmatrix}.$$

The construction of  $F$  through these tensors, which are computed exactly rather than by numerical integration, allows us to significantly reduce the computational complexity of the problem by taking advantage of the system's dynamics. We compute the approximate solution  $\pi^N$  first for a low-dimensional full-order model with  $n = 2$ , and then with high-dimensional full-order models with  $n = 100$  and  $n = 1000$ . In each of these cases, we test the solution over different domains  $\Omega = [-1, 1]^2$ ,  $\Omega = [-2, 2]^2$ , and  $\Omega = [-3, 3]^2$ , as well as for different maximum degrees  $M = 2$ ,  $M = 4$ , and  $M = 6$ . The error in each case is measured over the same subdomain  $W = [-0.7, 0.7]$ .

The resulting average residual error  $\|R(\mathbf{c}, \omega)\|_{(2, W)}$  for  $n = 2$  is shown in Table 3. In general, the error decreases with an increased maximum degree of the approximation, as the class of solutions for lower maximum degrees is contained in the class of solutions for higher degrees. The residual error increases when the domain  $\Omega$  is enlarged for the same degree of expansion. However, for the larger domains, the method still recovers a relatively good approximation of the mapping  $\pi$ , implying that the region  $W^0$  about the origin where the invariant is defined contains the rectangle  $[-3, 3]$ .

Domain	$M = 2$	$M = 4$	$M = 6$
$\Omega = [-1, 1]^2$	$1.3626 \times 10^{-3}$	$1.9130 \times 10^{-5}$	$7.0587 \times 10^{-7}$
$\Omega = [-2, 2]^2$	$8.2881 \times 10^{-3}$	$4.7759 \times 10^{-4}$	$7.9316 \times 10^{-5}$
$\Omega = [-3, 3]^2$	$2.1234 \times 10^{-2}$	$1.3698 \times 10^{-3}$	$7.1681 \times 10^{-4}$

Table 3: Table of the average residual error  $\|R(\mathbf{c}, \omega)\|_{(2, W)}$  over the subdomain  $W = [-0.7, 0.7]^2$  for different values of  $\Omega$  and  $M$  for the Galerkin approximation to the invariant mapping  $\pi$  with  $n = 2$  for the RL ladder problem with a linear oscillator signal generator with constants  $a = 2$  and  $\kappa = 1.1$ .

The corresponding results and residual error  $\|R(\mathbf{c}, \omega)\|_{(2, W)}$  for  $n = 100$  are shown in Table 4. Once again, we can see that the method recovers a similarly good approximation of the solution. The error is on the same order of magnitude as it is for  $n = 2$ , and is even slightly smaller in most cases. All tests are able to recover the mapping quite well with a maximum polynomial degree of 6. We also show the results for  $n = 1000$  in Table 5. We see similar results for  $n = 100$  and  $n = 1000$  for this test. This example demonstrates that the algorithm is able to recover the solution to 1000 dimensions for the RL ladder circuit with a linear oscillator as a signal generator.

To give a representative example of the computational cost of the algorithm, Table 6 shows the amount of time required for the algorithm to converge for  $\Omega = [-1, 1]^2$



Domain	$M = 2$	$M = 4$	$M = 6$
$\Omega = [-1, 1]^2$	$1.0617 \times 10^{-3}$	$2.2500 \times 10^{-5}$	$7.0723 \times 10^{-7}$
$\Omega = [-2, 2]^2$	$6.5405 \times 10^{-3}$	$5.8132 \times 10^{-4}$	$8.1913 \times 10^{-5}$
$\Omega = [-3, 3]^2$	$1.7266 \times 10^{-2}$	$1.7815 \times 10^{-3}$	$7.6927 \times 10^{-4}$

Table 4: Table of the average residual error  $\|R(\mathbf{c}, \omega)\|_{(2,W)}$  over the subdomain  $W = [-0.7, 0.7]^2$  for different values of  $\Omega$  and  $M$  for the Galerkin approximation to the invariant mapping  $\pi$  with  $n = 100$  for the RL ladder problem with a linear oscillator signal generator with a constants  $a = 2$  and  $\kappa = 1.1$ .

Domain	$M = 2$	$M = 4$	$M = 6$
$\Omega = [-1, 1]^2$	$1.0617 \times 10^{-3}$	$2.2500 \times 10^{-5}$	$7.0723 \times 10^{-7}$
$\Omega = [-2, 2]^2$	$6.5405 \times 10^{-3}$	$5.8132 \times 10^{-4}$	$8.1913 \times 10^{-5}$
$\Omega = [-3, 3]^2$	$1.7266 \times 10^{-2}$	$1.7815 \times 10^{-3}$	$7.6927 \times 10^{-4}$

Table 5: Table of the average residual error  $\|R(\mathbf{c}, \omega)\|_{(2,W)}$  over the subdomain  $W = [-0.7, 0.7]^2$  for different values of  $\Omega$  and  $M$  for the Galerkin approximation to the invariant mapping  $\pi$  with  $n = 1000$  for the RL ladder problem with a linear oscillator signal generator with a constants  $a = 2$  and  $\kappa = 1.1$ .

and  $M = 6$  for the different dimensions. All computations were carried out on a 2.3 GHz Quad-Core Intel i7 processor. The results show that even for 1000 dimensions, the problem is tractable for a Galerkin expansion in up to 6 dimensions on a laptop's processor.

	$n = 2$	$n = 100$	$n = 1000$
time (s)	7.1	447	6935

Table 6: Table showing the computational time, in seconds, required to compute the approximate solution  $\pi^N$  for  $n = 2, 100, 1000$ , with  $\Omega = [-1, 1]^2$  and  $M = 6$ .

Based on the computed  $\pi^N$  for these different cases, it remains to use this approximate invariant mapping to construct a stable reduced-order model to mirror the output of the nonlinear full-order system. We recall from (2.13) that we would like a reduced-order model of the form

$$\begin{aligned} \dot{r} &= s(r) - \bar{g}(r, \ell(r)) + \bar{g}(r, u) \\ y_r &= h(\pi(r)), \end{aligned}$$

where  $\bar{g}$  is a free mapping. As long as  $g(\cdot)$  is chosen so that the system is locally exponentially stable, the reduced-order model will achieve moment matching. **Sub-**

section 2.2 gave a way to construct this mapping in general, but for this particular case it can be shown that the mapping

$$(4.9) \quad \bar{g}(r, u) = \begin{bmatrix} 0 \\ c \end{bmatrix} u$$

achieves asymptotic stability for some sufficiently large, positive constant  $c$ , and can therefore be used to construct the reduced-order model. This reduced-order model is given by

$$(4.10) \quad \begin{aligned} \dot{r} &= s(r) - \begin{bmatrix} 0 \\ c \end{bmatrix} \ell(r) + \begin{bmatrix} 0 \\ c \end{bmatrix} u \\ y_r &= h(\pi^N(r)) \end{aligned}$$

for our approximate solution  $\pi^N$  to the invariant mapping. We can compare its steady-state output to the steady-state output of the full-order model. To compare the results, we numerically solve the interconnected system in time for both the full-order model and the reduced-order model, and compare the outputs  $y(t)$  and  $y_r(t)$ . In order to simulate these, arbitrary initial conditions must be chosen for  $\omega_0$  in the signal generating system and for  $r_0$  in the reduced-order model. Figure 2 shows both outputs for the case  $n = 1000$ , for the mapping  $\pi^N$  found on the domain  $\Omega = [-1, 1]^2$  with a maximum degree  $M = 6$ , over the time period  $t \in [0, 10]$ . This test was carried out for an initial condition of  $\omega_0 = (0.1, 0.2)^\top$  and arbitrarily chosen starting points of  $r_0 = (0, 1)^\top$  and  $x_0 = 0$  for the reduced-order model system and the full-order model system, respectively. When constructing the reduced-order model, we use the constant  $c = 10$ . We can see that we are able to recover the full-order model signal using the reduced-order model, and accurately achieve moment matching for this problem.

We can measure how well the reduced-order model approximates the steady-state response of the system by measuring the RMS error of the response after both the full-order model and reduced-order model signals reach the steady-state. We can then divide this error by the amplitude of the signal to obtain a measure of how well the reduced-order model matches the steady-state response. The RMS error is observed after the simulation reaches steady-state behaviour. Table 7, Table 8, and Table 9 show the relative error for each of the different conditions tested.

We can see that all conditions are able to accurately approximate the steady-state response for  $n = 2$ ,  $n = 100$ , and  $n = 1000$ . The performance decreases slightly for the higher dimensional problem, but the difference is not particularly large, and the RMS error is below 0.5 percent for a maximum degree of 6 in all cases, showing that the reduced-order model approximates the full-order model, even when its dimensionality is much less than that of the full-order model.

**4.5. Test 4: Nonlinear resistor-inductor ladder with Van der Pol oscillator as signal generator.** We now consider an example with a nonlinear signal generator. We use the Van der Pol oscillator as the signal generator, modeled as

$$(4.11) \quad s(\omega) = \begin{bmatrix} \omega_2 \\ -\omega_1 + \mu(1 - \omega_1^2)\omega_2 \end{bmatrix} \quad \ell(\omega) = \omega_2 \quad \mu > 0.$$

The system is the same RL ladder circuit represented in (4.3). We use the same tensors  $\mathbf{N}$  and  $\mathbf{O}$  as in Test 3, and  $\mathbf{A}$  is now constructed using the new signal generator

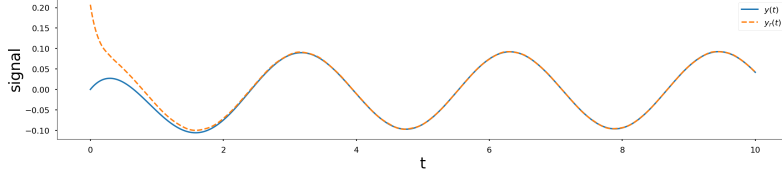
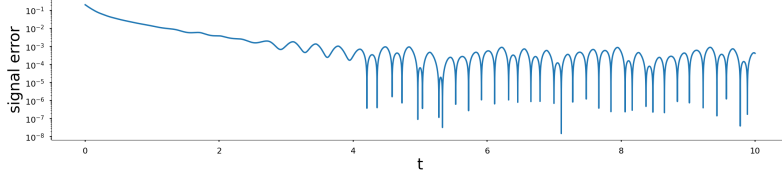
(a) plot of  $y(t)$  vs.  $y_r(t)$ , with  $\Omega = [-1, 1]^2$ ,  $n = 1000$ .(b) plot of  $|y(t) - y_r(t)|$ , with  $\Omega = [-1, 1]^2$ ,  $n = 1000$ .

Fig. 2: Plot of  $y(t)$  and  $y_r(t)$  for  $t \in [0, 50]$  for the RL ladder problem with a linear oscillator signal generator for a domain  $\Omega = [-1, 1]^2$  and a maximum degree  $M = 6$  for the dimension  $n = 1000$ , with constants  $a = 2$ ,  $\kappa = 1.1$ ,  $c = 10$  and initial conditions  $\omega_0 = (0.1, 0.2)^\top$ ,  $r_0 = (0, 1)^\top$  and  $x_0 = 0$ .

Domain	$M = 2$	$M = 4$	$M = 6$
$\Omega = [-1, 1]^2$	$3.2250 \times 10^{-3}$	$3.5399 \times 10^{-4}$	$3.4580 \times 10^{-4}$
$\Omega = [-2, 2]^2$	$1.4806 \times 10^{-2}$	$9.6175 \times 10^{-4}$	$3.9628 \times 10^{-4}$
$\Omega = [-3, 3]^2$	$3.6235 \times 10^{-2}$	$1.7328 \times 10^{-3}$	$1.4298 \times 10^{-3}$

Table 7: Table of the relative steady-state RMS error of the reduced-order model with  $n = 2$  for the RL ladder problem with a linear oscillator signal generator with a constants  $a = 2$  and  $\kappa = 1.1$ .

Domain	$M = 2$	$M = 4$	$M = 6$
$\Omega = [-1, 1]^2$	$3.2222 \times 10^{-3}$	$1.5413 \times 10^{-3}$	$1.5371 \times 10^{-3}$
$\Omega = [-2, 2]^2$	$1.3348 \times 10^{-2}$	$1.9930 \times 10^{-3}$	$1.5520 \times 10^{-3}$
$\Omega = [-3, 3]^2$	$3.5621 \times 10^{-2}$	$3.2516 \times 10^{-3}$	$2.2785 \times 10^{-3}$

Table 8: Table of the relative steady-state RMS error of the reduced-order model with  $n = 100$  for the RL ladder problem with a linear oscillator signal generator with constants  $a = 2$  and  $\kappa = 1.1$ .

described by  $s(\omega)$  in (4.11). Using this new  $\mathbf{A}$  and  $Q$ , we get the same expressions for

Domain	$M = 2$	$M = 4$	$M = 6$
$\Omega = [-1, 1]^2$	$5.3946 \times 10^{-3}$	$4.4702 \times 10^{-3}$	$4.4676 \times 10^{-3}$
$\Omega = [-2, 2]^2$	$1.4154 \times 10^{-2}$	$4.6679 \times 10^{-3}$	$4.4713 \times 10^{-3}$
$\Omega = [-3, 3]^2$	$3.3966 \times 10^{-2}$	$5.4216 \times 10^{-3}$	$4.7748 \times 10^{-3}$

Table 9: Table of the relative steady-state RMS error of the reduced-order model with  $n = 1000$  for the RL ladder problem with a linear oscillator signal generator with constants  $a = 2$  and  $\kappa = 1.1$ .

$F_i$  as shown in (4.7) and for  $JF$  as in (4.8).

We compute the solution to the invariance equation with a constant value of  $\mu = 0.25$  and  $\kappa = 1.1$ . Table 10 shows the resulting error  $\|R(\mathbf{c}, \omega)\|_{(2,W)}$  for the case  $n = 2$ , averaged over the subdomain  $W = [-0.7, 0.7]^2$ . Once again, we can see that a higher maximum degree results in a better approximation, but the solution deteriorates as the domain  $\Omega$  increases.

Domain	$M = 2$	$M = 4$	$M = 6$
$\Omega = [-1, 1]^2$	$8.0711 \times 10^{-3}$	$4.1311 \times 10^{-4}$	$2.8741 \times 10^{-5}$
$\Omega = [-2, 2]^2$	$3.9200 \times 10^{-2}$	$2.6989 \times 10^{-2}$	$7.0562 \times 10^{-2}$
$\Omega = [-3, 3]^2$	$1.0014 \times 10^{-1}$	$3.2736 \times 10^{-1}$	$1.5181 \times 10^{-1}$

Table 10: Table of the average residual error  $\|R(\mathbf{c}, \omega)\|_{(2,W)}$  over the subdomain  $W = [-0.7, 0.7]^2$  for different values of  $\Omega$  and  $M$  for the Galerkin approximation to the invariant mapping  $\pi$  with  $n = 2$  for the RL ladder problem with a Van der Pol oscillator signal generator with constants  $\mu = 0.25$  and  $\kappa = 1.1$ .

Table 11 shows the corresponding results for the higher dimensional  $n = 100$ . For the smaller domains  $\Omega = [-1, 1]^2$  and  $\Omega = [-2, 2]^2$ , the results are similar to the previous tests, and the error decreases with a larger maximum degree of the expansion, indicating that the higher maximum degree is better able to approximate the solution to the PDE system. The algorithm failed to converge within 300 iterations for the higher maximum degrees on the domain of  $\Omega = [-3, 3]^2$ . Since the signal generator in this example is nonlinear, it is possible that the domain  $W^0$  where the mapping is valid is smaller than in the case of the linear signal generator; because the nonlinearity contains a monomial of degree 3 in  $\mu\omega_1^2\omega_2$ , a larger domain will amplify any error near the edges of the domain, and small errors in  $\pi^N$  will cause large errors in  $\|R(\mathbf{c}, \omega)\|_{(2,W)}$ . The results for  $n = 1000$  are shown in Table 12. These results are once again very similar to those for  $n = 100$ , and show a good approximation for a domain size up to  $\Omega = [-2, 2]^2$ , with the algorithm also failing to converge within 300 iterations on the larger domain.

Table 13 shows the amount of computational time required for the algorithm to converge for  $\Omega = [-1, 1]^2$  and  $M = 6$  for different dimensions.

Domain	$M = 2$	$M = 4$	$M = 6$
$\Omega = [-1, 1]^2$	$6.0786 \times 10^{-3}$	$2.9373 \times 10^{-4}$	$2.0639 \times 10^{-5}$
$\Omega = [-2, 2]^2$	$5.0803 \times 10^{-2}$	$9.7273 \times 10^{-3}$	$1.1899 \times 10^{-2}$
$\Omega = [-3, 3]^2$	$4.0017 \times 10^{-2}$	-	-

Table 11: Table of the average residual error  $\|R(\mathbf{c}, \omega)\|_{(2, W)}$  over the subdomain  $W = [-0.7, 0.7]^2$  for different values of  $\Omega$  and  $M$  for the Galerkin approximation to the invariant mapping  $\pi$  with  $n = 100$  for the RL ladder problem with a Van der Pol oscillator signal generator with a constants  $\mu = 0.25$  and  $\kappa = 1.1$ .

Domain	$M = 2$	$M = 4$	$M = 6$
$\Omega = [-1, 1]^2$	$6.0786 \times 10^{-3}$	$2.9373 \times 10^{-4}$	$2.0639 \times 10^{-5}$
$\Omega = [-2, 2]^2$	$5.0662 \times 10^{-2}$	$4.0561 \times 10^{-2}$	$9.0314 \times 10^{-3}$
$\Omega = [-3, 3]^2$	$3.8131 \times 10^{-2}$	-	-

Table 12: Table of the average residual error  $\|R(\mathbf{c}, \omega)\|_{(2, W)}$  over the subdomain  $W = [-0.7, 0.7]^2$  for different values of  $\Omega$  and  $M$  for the Galerkin approximation to the invariant mapping  $\pi$  with  $n = 1000$  for the RL ladder problem with a Van der Pol oscillator signal generator with a constants  $\mu = 0.25$  and  $\kappa = 1.1$ .

	$n = 2$	$n = 100$	$n = 1000$
time (s)	10.6	438	6955

Table 13: Table showing the computational time, in seconds, required to compute the approximate solution  $\pi^N$  for  $n = 2, 100, 1000$ , with  $\Omega = [-1, 1]^2$  and  $M = 6$ .

We once again want to find an expression for the reduced-order model based on the computed  $\pi^N$ . We use a similar approach as we do in the previous example with the linear oscillator signal generator, and this time we use the mapping

$$(4.12) \quad \bar{g}(r, u) = \begin{bmatrix} 0 \\ \mu(1 - r_1^2) + c \end{bmatrix} u$$

for some sufficiently large, positive constant  $c$ . This mapping achieves exponential stability for the resulting reduced-order model, given as

$$(4.13) \quad \begin{aligned} \dot{r} &= s(r) - \begin{bmatrix} 0 \\ \mu(1 - r_1^2) + c \end{bmatrix} \ell(r) + \begin{bmatrix} 0 \\ \mu(1 - r_1^2) + c \end{bmatrix} u \\ y_r &= h(\pi^N(r)) \end{aligned}$$

for our approximate solution  $\pi^N$  to the invariant mapping.

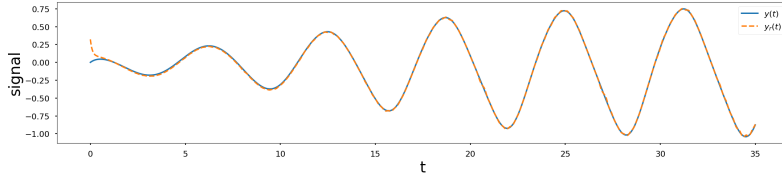
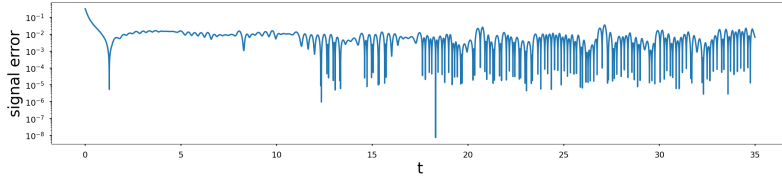
(a) plot of  $y(t)$  vs.  $y_r(t)$ , with  $\Omega = [-1, 1]^2$ ,  $n = 1000$ .(b) plot of  $|y(t) - y_r(t)|$ , with  $\Omega = [-1, 1]^2$ ,  $n = 1000$ .

Fig. 3: Plot of  $y(t)$  and  $y_r(t)$  for  $t \in [0, 50]$  for the RL ladder problem with a Van der Pol oscillator signal generator for a domain  $\Omega = [-1, 1]^2$  and a maximum degree  $M = 4$  for the dimension  $n = 1000$ , with constants  $\mu = 0.25, \kappa = 1.1, c = 10$  and initial conditions  $\omega_0 = (0.1, 0.2)^\top$ ,  $r_0 = (0, 1)^\top$  and  $x_0 = 0$ .

The steady-state output of the reduced-order model is compared to the steady-state output of the full-order model. Figure 3 shows the output of the full-order model in blue and the output of the reduced-order model in red for the case  $n = 1000$ . Similarly to the case of the linear signal generator, the test is carried out for  $\Omega = [-1, 1]^2$  with  $M = 6$  with initial conditions  $\omega_0 = (0.1, 0.2)^\top$ ,  $r_0 = (0, 1)^\top$  and  $x_0 = 0$ , over the time period  $t \in [0, 35]$ . We use a constant of  $c = 10$ . In this case, the model is able to recover the steady-state behaviour of the full-order system for  $n = 1000$ . The figures are very similar for  $n = 2$  and  $n = 100$ , which are not shown.

Once again, we evaluate the reduced-order model approximation by looking at the relative RMS error of the steady-state response. The RMS error is observed after the simulation reaches steady-state behaviour. Table 14, Table 15 and Table 16 show the relative error for each of the different conditions tested.

In the case of the Van der Pol oscillator, we see that for  $n = 2$  the performance of the reduced-order model is once again quite similar for most of the conditions, and we get a relatively good approximation of the steady-state response. Higher polynomial expansions result in lower RMS error. In the case of  $n = 100$  and  $n = 1000$ , the higher dimensional expansions all behave quite well for  $\Omega = [-1, 1]^2$  and  $\Omega = [-2, 2]^2$ . The RMS error is low in these cases, showing that the reduced-order model remains able to recover the steady-state behaviour of the full-order system in these higher dimensional cases for the Van der Pol oscillator.

**5. Concluding remarks.** This paper presents a technique for approximating the solution of the invariance PDE system that arises from reduced-order modeling via moment matching for nonlinear systems. These findings for approximating the moment of a system can be applicable to model order reduction problems, as well as immersion and invariance techniques. The solution to the system of PDEs is approximated using a spectral expansion through a chosen set of basis functions. The

Domain	$M = 2$	$M = 4$	$M = 6$
$\Omega = [-1, 1]^2$	$4.5723 \times 10^{-2}$	$7.7093 \times 10^{-3}$	$1.6723 \times 10^{-3}$
$\Omega = [-2, 2]^2$	$5.1643 \times 10^{-2}$	$1.9637 \times 10^{-2}$	$4.9413 \times 10^{-2}$
$\Omega = [-3, 3]^2$	$1.2946 \times 10^{-1}$	$2.0774 \times 10^{-1}$	$5.7344 \times 10^{-2}$

Table 14: Table of the relative steady-state RMS error of the reduced-order model with  $n = 2$  for the RL ladder problem with a Van der Pol oscillator signal generator with constants  $\mu = 0.25$  and  $\kappa = 1.1$ .

Domain	$M = 2$	$M = 4$	$M = 6$
$\Omega = [-1, 1]^2$	$4.3206 \times 10^{-2}$	$7.1173 \times 10^{-3}$	$3.4599 \times 10^{-3}$
$\Omega = [-2, 2]^2$	$3.0439 \times 10^{-1}$	$1.5848 \times 10^{-2}$	$5.5036 \times 10^{-3}$
$\Omega = [-3, 3]^2$	$3.2542 \times 10^{-1}$	-	-

Table 15: Table of the relative steady-state RMS error of the reduced-order model with  $n = 100$  for the RL ladder problem with a Van der Pol oscillator signal generator with constants  $\mu = 0.25$  and  $\kappa = 1.1$ .

Domain	$M = 2$	$M = 4$	$M = 6$
$\Omega = [-1, 1]^2$	$4.3949 \times 10^{-2}$	$8.1825 \times 10^{-3}$	$5.7352 \times 10^{-3}$
$\Omega = [-2, 2]^2$	$3.0441 \times 10^{-1}$	$1.6432 \times 10^{-2}$	$6.9633 \times 10^{-3}$
$\Omega = [-3, 3]^2$	$3.2592 \times 10^{-1}$	-	-

Table 16: Table of the relative steady-state RMS error of the reduced-order model with  $n = 1000$  for the RL ladder problem with a Van der Pol oscillator signal generator with constants  $\mu = 0.25$  and  $\kappa = 1.1$ .

algorithm to find an approximate solution to this problem can be greatly sped up by constructing matrices and tensors taking advantage of the problem's structure. Numerical tests are able to find approximate solutions to the invariance PDE system and recover the behaviour of the steady-state responses of the full-order models for nonlinear systems of dimension up to  $n = 1000$ . In cases where an analytical solution exists, the method is able to recover the exact solution in the polynomial basis. In more complex cases, the algorithm can build a reduced-order model that achieves moment matching and produces a good approximation to the steady-state behaviour of the full-order model. '

A potential future direction to take this research involves using signal generators of higher dimensionality. Currently, we have considered signal generators of dimen-

sion  $d = 2$ , which means that our method only involves the computation of two-dimensional integrals in the evaluation of the function  $F$ . Using higher-dimensional signal generators would allow us to create reduced-order models for problems with more complex input signals, capturing richer dynamical behaviour. In particular, the ability to handle higher-dimensional signal generators could be especially helpful in analyzing multi-input, multi-output systems. Increasing the dimensionality of the signal generator also introduces formidable computational challenges, as leading to large-scale systems of high-dimensional PDEs. In some cases, it may be possible to leverage the problem's structure in order to compute these, for example if the system's dynamics are separable.

## REFERENCES

- [1] A. ANTOUNAS, *An overview of approximation methods for large-scale dynamical systems*, Annual Reviews in Control, 29 (2005), pp. 181–190, <https://doi.org/10.1016/j.arcontrol.2005.08.002>.
- [2] A. C. ANTOUNAS, *Approximation of Large-Scale Dynamical Systems*, Society for Industrial and Applied Mathematics, 2005, <https://doi.org/10.1137/1.9780898718713>.
- [3] A. ASTOLFI, *Model reduction by moment matching for nonlinear systems*, in 2008 47th IEEE Conference on Decision and Control, 2008, pp. 4873–4878, <https://doi.org/10.1109/CDC.2008.4738791>.
- [4] A. ASTOLFI, *Model reduction by moment matching for linear and nonlinear systems*, IEEE Transactions on Automatic Control, 55 (2010), pp. 2321–2336, <https://doi.org/10.1109/TAC.2010.2046044>.
- [5] A. ASTOLFI AND R. ORTEGA, *Immersion and invariance: a new tool for stabilization and adaptive control of nonlinear systems*, IEEE Transactions on Automatic Control, 48 (2003), pp. 590–606, <https://doi.org/10.1109/TAC.2003.809820>.
- [6] B. AZMI, D. KALISE, AND K. KUNISCH, *Optimal feedback law recovery by gradient-augmented sparse polynomial regression*, Journal of Machine Learning Research, 22 (2021), pp. 1–32, <http://jmlr.org/papers/v22/20-755.html>.
- [7] R. W. BEARD, *Improving the Closed-Loop Performance of Nonlinear Systems*, PhD thesis, Rensselaer Polytechnic Institute, 1995.
- [8] R. W. BEARD, G. N. SARIDIS, AND J. T. WEN, *Galerkin approximations of the generalized Hamilton-Jacobi-Bellman equation*, Automatica, 33 (1997), pp. 2159–2177, [https://doi.org/10.1016/S0005-1098\(97\)00128-3](https://doi.org/10.1016/S0005-1098(97)00128-3).
- [9] R. BELLMAN, *Adaptive Control Processes: A Guided Tour*, Princeton University Press, 1961, <http://www.jstor.org/stable/j.ctt183ph6v> (accessed 2023-10-27).
- [10] P. BENNER AND P. GOYAL, *Interpolation-based model order reduction for polynomial parametric systems*, 2019, <https://arxiv.org/abs/1904.11891>.
- [11] P. BENNER, W. SCHILDERS, S. GRIVET-TALOCIA, A. QUARTERONI, G. ROZZA, AND L. MIGUEL SILVEIRA, *Model Order Reduction: Volume 3 Applications*, De Gruyter, 2020, <https://doi.org/10.1515/9783110499001>.
- [12] C. I. BYRNES AND A. ISIDORI, *Limit sets, zero dynamics, and internal models in the problem of nonlinear output regulation*, IEEE Transactions on Automatic Control, 48 (2003), pp. 1712–1723.
- [13] J. CARR, *Applications of Centre Manifold Theory*, Springer-Verlag New York Inc., 1981, <https://doi.org/10.1007/978-1-4612-5929-9>.
- [14] N. FAEDO, G. SCARCIOTTI, A. ASTOLFI, AND J. V. RINGWOOD, *On the approximation of moments for nonlinear systems*, IEEE Transactions on Automatic Control, 66 (2021), pp. 5538–5545, <https://doi.org/10.1109/TAC.2021.3054325>.
- [15] K. GALLIVAN, A. VANDENDORPE, AND P. VAN DOOREN, *Sylvester equations and projection-based model reduction*, Journal of Computational and Applied Mathematics, 162 (2004), pp. 213–229, <https://doi.org/10.1016/j.cam.2003.08.026>. Proceedings of the International Conference on Linear Algebra and Arithmetic 2001.
- [16] W. GRAY AND J. SCHERPEN, *Nonlinear Hilbert adjoints: properties and applications to Hankel singular value analysis*, in Proceedings of the 2001 American Control Conference., vol. 5, 2001, pp. 3582–3587, <https://doi.org/10.1109/ACC.2001.946190>.
- [17] W. GRAY AND E. VERRIEST, *Balanced realizations near stable invariant manifolds*, Automatica, 42 (2006), pp. 653–659, <https://doi.org/10.1016/j.automatica.2005.12.007>.



- [18] R. HERMANN AND A. KRENER, *Nonlinear controllability and observability*, IEEE Transactions on Automatic Control, 22 (1977), pp. 728–740, <https://doi.org/10.1109/TAC.1977.1101601>.
- [19] T. C. IONESCU AND A. ASTOLFI, *Nonlinear moment matching-based model order reduction*, IEEE Transactions on Automatic Control, 61 (2015), pp. 2837–2847.
- [20] A. ISIDORI, *Nonlinear Control Systems*, Springer London, 3 ed., 1995, <https://doi.org/10.1007/978-1-84628-615-5>.
- [21] A. ISIDORI AND C. I. BYRNES, *Steady-state behaviors in nonlinear systems with an application to robust disturbance rejection*, Annual Reviews in Control, 32 (2008), pp. 1–16, <https://doi.org/10.1016/j.arcontrol.2008.01.001>.
- [22] D. KALISE, S. KUNDU, AND K. KUNISCH, *Robust feedback control of nonlinear PDEs by numerical approximation of high-dimensional Hamilton-Jacobi-Isaacs equations*, 2019, <https://arxiv.org/abs/1905.06276>.
- [23] D. KALISE AND K. KUNISCH, *Polynomial approximation of high-dimensional hamilton-jacobi-bellman equations and applications to feedback control of semilinear parabolic pdes*, SIAM Journal on Scientific Computing, 40 (2017), <https://doi.org/10.1137/17M1116635>.
- [24] Y. KAWANO AND J. M. SCHERPEN, *Empirical differential gramians for nonlinear model reduction*, Automatica, 127 (2021), p. 109534, <https://doi.org/10.1016/j.automatica.2021.109534>.
- [25] H. KHALIL, *Nonlinear Systems*, Always Learning, Pearson, 2015, <https://books.google.co.uk/books?id=Gt2HAQAACAAJ>.
- [26] B. KRAMER, S. GUGERCIN, AND J. BORGGAARD, *Nonlinear balanced truncation: Part 2 – model reduction on manifolds*, 2023, <https://arxiv.org/abs/2302.02036>.
- [27] B. KRAMER, S. GUGERCIN, J. BORGGAARD, AND L. BALICKI, *Nonlinear balanced truncation: Part 1-computing energy functions*, 2022, <https://arxiv.org/abs/2209.07645>.
- [28] K. KUNISCH AND S. VOLKWEIN, *Control of the burgers equation by a reduced-order approach using proper orthogonal decomposition*, Journal of Optimization Theory and Applications, 102 (1999), pp. 345–371, <https://api.semanticscholar.org/CorpusID:118949739>.
- [29] K. KUNISCH AND S. VOLKWEIN, *Proper orthogonal decomposition for optimality systems*, ESAIM: Mathematical Modelling and Numerical Analysis, 42 (2008), pp. 1–23, <http://eudml.org/doc/250374>.
- [30] A. MORESCHINI AND A. ASTOLFI, *Closed-loop interpolation by moment matching for linear and nonlinear systems*, IEEE Transaction on Automatic Control, (2025), <https://doi.org/10.1109/TAC.2024.3484309>. (Early Access).
- [31] A. MORESCHINI, M. SCANDELLA, AND T. PARISINI, *Nonlinear data-driven moment matching in Reproducing Kernel Hilbert Spaces*, in Eur. Control Conf. (ECC), 2024, pp. 3440–3445, <https://doi.org/10.23919/ECC64448.2024.10590737>.
- [32] R. ORTEGA, B. YI, J. G. ROMERO, AND A. ASTOLFI, *Orbital stabilization of nonlinear systems via the immersion and invariance technique*, International Journal of Robust and Nonlinear Control, 30 (2020), pp. 1850–1871, <https://doi.org/10.1002/rnc.4861>.
- [33] D. RAFIQ AND M. A. BAZAZ, *Model order reduction via moment-matching: A state of the art review*, Archives of Computational Methods in Engineering, (2022), <https://doi.org/10.1007/s11831-021-09618-2>.
- [34] M. REWIENSKI AND J. WHITE, *A trajectory piecewise-linear approach to model order reduction and fast simulation of nonlinear circuits and micromachined devices*, IEEE Transactions on Computer-Aided Design of Integrated Circuits and Systems, 22 (2003), pp. 155–170, <https://doi.org/10.1109/TCAD.2002.806601>.
- [35] G. SCARCIOTTI AND A. ASTOLFI, *Data-driven model reduction by moment matching for linear and nonlinear systems*, Automatica, 79 (2017), pp. 340–351.
- [36] G. SCARCIOTTI AND A. ASTOLFI, *Interconnection-based model order reduction-a survey*, European Journal of Control, 75 (2024), p. 100929.
- [37] J. SCHERPEN AND W. GRAY, *Minimality and local state decompositions of a nonlinear state space realization using energy functions*, IEEE Transactions on Automatic Control, 45 (2000), pp. 2079–2086, <https://doi.org/10.1109/9.887630>.
- [38] J. M. A. SCHERPEN, *Balancing for nonlinear systems*, Systems & Control Letters, 21 (1993), pp. 143–153.
- [39] J. D. SIMARD, A. MORESCHINI, AND A. ASTOLFI, *Parameterization of all moment matching interpolants*, in European Control Conference (ECC), 2023, pp. 1–6, <https://doi.org/10.23919/ECC57647.2023.10178406>.
- [40] J. D. SIMARD, A. MORESCHINI, AND A. ASTOLFI, *Parameterization of all differential-algebraic moment matching interpolants*, IEEE Transactions on Automatic Control, (2024), <https://doi.org/10.1109/TAC.2024.3469247>. (Early Access).

- [41] H. J. SUSSMANN AND V. JURDJEVIC, *Controllability of nonlinear systems*, Journal of Differential Equations, 12 (1972), pp. 95–116, [https://doi.org/https://doi.org/10.1016/0022-0396\(72\)90007-1](https://doi.org/https://doi.org/10.1016/0022-0396(72)90007-1), <https://www.sciencedirect.com/science/article/pii/0022039672900071>.
- [42] K. WILLCOX AND J. PERAIRE, *Balanced model reduction via the proper orthogonal decomposition*, AIAA Journal, 40 (2002), pp. 2323–2330, <https://doi.org/10.2514/2.1570>.